

Material Injection Alleviation during the RAM C-III Flight

LYLE C. SCHROEDER* AND NORMAN D. AKEY*

NASA Langley Research Center, Hampton, Va.

The results of a material injection RF blackout alleviation experiment and of plasma diagnostic measurements using electrostatic probes and an S-band reflectometer in a 25,000 fps re-entry flight are presented. Significant alleviation of RF blackout is observed at altitudes of from 270,000 ft to 120,000 ft due to injection of water and Freon E-3 on VHF, S-band, C-band, and X-band frequencies. Electrostatic probe data, attenuation data, and S-band diagnostic data show consistent plasma results. The relative effectiveness of water and Freon E-3 is discussed.

Introduction

THIS paper describes results of the last flight in a series conducted in the NASA Langley Research Center's Radio Attenuation Measurements (RAM) program. The RAM A and B re-entry blackout experiments were conducted on hemispherically blunted conical spacecraft with nose radii of 1 and 4 in., respectively, at entry velocities of 18,000 fps.¹ The RAM C series configuration was a 6-in.-radius, hemispherically blunted, 9° half-angle cone which re-entered at 25,000 fps. RAM C-I, the first flight of the series, yielded diagnostic plasma measurements using Langmuir probes extending into the flowfield and data showing the effectiveness of water injection alleviation during the radio blackout.² RAM C-II, the second flight,³ provided diagnostic plasma measurements with no ablation contaminant impurities in the flow field using microwave reflectometers at four frequencies at many body stations, and using Langmuir probes as on C-I.

RAM C-III was the final flight, and this paper primarily focuses on the key objective, the alleviation of radio blackout by injection of water and Freon E-3. The degree of alleviation was principally determined by the effects of injection on the attenuation of the 259.7 MHz VHF telemetry antenna. Effects of injection on attenuation at other frequencies and on S-band and electrostatic probe measurements are also discussed. (Details of the Langmuir probe results of RAM C-III are discussed in a paper by Kang, Jones, and Dunn.⁴)

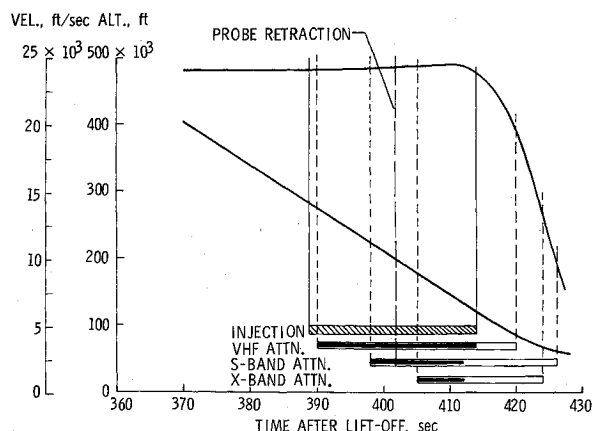


Fig. 1 RAM C-III profile and data period. (Dark bar within attenuation band indicates times when injection effects were observed.)

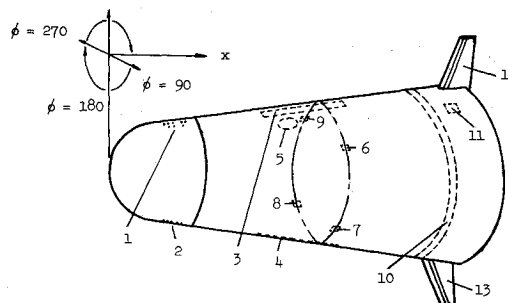
Description of Systems

1. Launch and Flight Systems

The RAM C-III flight was conducted using a four-stage Scout launch vehicle. The re-entry trajectory flown by RAM C-III is given in Fig. 1. This trajectory was similar by design to that of RAM C-I and C-II to enable comparison of the experiment results of all three flights. The attenuation period and the injection period are indicated on this figure.

2. Re-Entry Payload

An illustration of the RAM C-III payload and the detailed location of RF system antennas and experiment system parts is given in Fig. 2. The major plasma diagnostic instruments, the S-band diagnostic antenna and the electrostatic probes, are indicated in the illustration. The injection orifice sites just aft of the nose are also shown. Notice that the electrostatic probes and the prime experiment antennas, the 259.7 MHz slots, are directly in line with the injection sites, and all other RF and diagnostic systems are at some other angle. The spacecraft nose cap was made of a carbon phenolic material containing 5000 ppm alkali



| Number | Part Function | x, (cm) | | ϕ deg (a) | x/D (b) |
|--------|--------------------------------------|---------|---------|----------------------|------------|
| | | in. | (cm) | | |
| 1 | Material injection site: Side 1 | 7.35 | (18.67) | 0 | .59 |
| 2 | Side 2 | 7.35 | (18.67) | 180 | .59 |
| 3 | Antenna: VHF slot (259.7 Mhz) | 29.6 | (75.2) | 0 | 2.36 |
| 4 | VHF slot (259.7 Mhz) | 29.6 | (75.2) | 180 | 2.36 |
| 5 | S-Band antenna (3348 Mhz) | 29.38 | (74.6) | 323 | 2.34 |
| 6 | X-Band horn (9210 Mhz) | 32.6 | (82.8) | 60 | 2.60 |
| 7 | X-Band horn (9210 Mhz) | 32.6 | (82.8) | 150 | 2.60 |
| 8 | X-Band horn (9210 Mhz) | 32.6 | (82.8) | 240 | 2.60 |
| 9 | X-Band horn (9210 Mhz) | 32.6 | (82.8) | 330 | 2.60 |
| 10 | VHF ring (230.4 Mhz) | 43.0 | (109.2) | --- | 3.42 |
| 11 | C-Band horn (5700 Mhz) | 46.6 | (118.4) | 30 | 3.71 |
| 12 | Probe: Electrostatic (Fixed Bias) | 48.6 | (123.4) | 0 | 3.87 |
| 13 | (Swept Bias) | 48.6 | (123.4) | 180 | 3.87 |

^aCenter-line location of parts.

^bNose diameter D is 12.56 in. (31.90 cm).

Fig. 2 Position of RF antennas and experiment components on the RAM C-III spacecraft.

Presented as Paper 72-690 at the AIAA 5th Fluid and Plasma Dynamics Conference, Boston, Mass., June 26-28, 1972; submitted July 14, 1972; revision received November 20, 1972.

Index categories: Spacecraft Communication Systems; Re-Entry Vehicle Testing; Launch Vehicle and Missile Guidance Systems (Including Command and Information Systems).

* Aerospace Technologist, Microwave Techniques Section, Telemetry Research Branch, Flight Instrumentation Division.

impurities, which can increase plasma density levels during periods of ablation. The aft part of the spacecraft was covered by Teflon.

3. Material Injection Experiment

The purpose of this experiment was to measure and compare the effectiveness of a liquid electrophilic (Freon E-3) and water in alleviating entry radio blackout. The mechanisms for producing electron density reduction (and hence, signal recovery from blackout) are theoretically quite different for water and an electrophilic. Water injection has been shown to produce signal recovery by causing enhanced recombination of electrons and ions at the surface of water droplets,⁵ while electrophilics reduce electron density by attaching electrons.⁶

Alleviation using water injection techniques has been already demonstrated in flight.^{2,7,8} However, the signal recovery during the most similar flight, RAM C-I,² was below expectations in magnitude and duration, and improper injectant penetration was the suspected cause. Following RAM C-I, extensive studies of injection penetration and distribution were conducted using large-scale models of the RAM C-III in several wind tunnels.⁹ The improved penetration control established in these studies provided the basis for the design of a more efficient injection system which was incorporated in RAM C-III.

Alleviation using electrophilic materials has been discussed in the literature in many instances, for example, Crowe and Kilpatrick.¹⁰ Many researchers felt that electrophilic materials were potentially superior to water in producing electron density reductions, but questioned its effectiveness at the high temperature of spacecraft entry. Recently, data obtained in a high-temperature (4000°K) laboratory plasma⁶ indicated electrophilic materials produced electron density reduction 10 times greater than water. To test these results in a re-entry flight environment, the injection experiment was flown on RAM C-III.

The electrophilic material selected for the flight experiment was Freon E-3 [$F(C_3F_6O)_3CH_2CF_3$]. This material was selected on the basis of its electron density reduction performance in air arc jets and in the high-temperature combustion plasma, and also because of its desirable injection properties.⁶

The RAM C-III experiment was designed to alternately inject both fluids, water and Freon E-3, into the flowfield with nearly the same penetration distances and mass flow rates, while measurements were made of the corresponding reduction in RF signal attenuation and electron and ion density. The material injection system used pressurized nitrogen to expel the liquid injectants through a network of fixed orifices that were programed with solenoid valves. A programed rise of injection pressure during the injection period was produced by controlling the opening time and size of control orifices. The injection pressure so obtained was matched to requirements calculated from wind-tunnel correlations of penetration with injection parameters.⁹ Two different flow rates (low and high) for each fluid were pulsed into the flow field in the sequence shown in the top plot of Fig. 3. The injection pulses were 0.2 sec long, with 0.3 sec between pulses. An additional 0.5 sec off period occurred at the end of each cycle, such that each cycle was 2.5 sec long. Ten such injection cycles occurred during the injection period.

4. Diagnostic Systems

a. Electrostatic probes

The electrostatic probes were located at the base of the spacecraft on a fin which projected 14 cm long into the flowfield. The plasma profile was observed by monitoring the ion and electron current at discrete locations of these probes. The probes extended twice as far into the flowfield as on the previous RAM C flights, since the prior measurements showed the peak plasma density occurred beyond 7 cm.¹¹ Probe measurements were taken about 20 times a second until the spacecraft descended to 200,000 ft, when the probes were retracted.

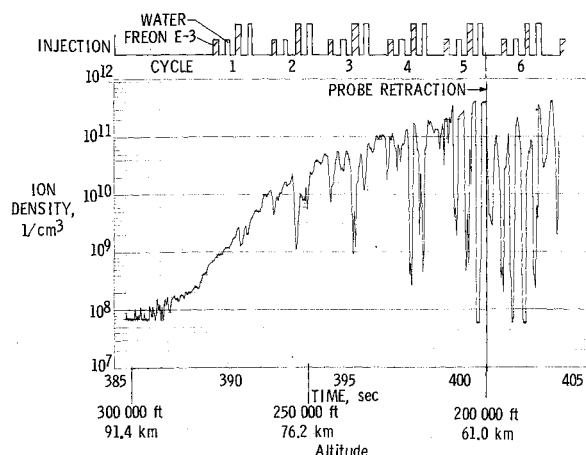


Fig. 3 Positive ion current measurements as a function of altitude and time for a single fixed-bias probe.

Two different types of probes were flown on RAM C-III. Probes with a bias voltage fixed so that only positive ion current is collected (which is related to plasma density) were installed in one probe. Probes with a bias voltage swept to obtain a complete voltage-current probe characteristic were installed in the other fin. The probe measurements yielded electron density, positive ion density, and electron temperature and are presented in more detail elsewhere.^{4,12}

b. S-Band antenna

The location of the S-band diagnostic antenna is shown in Fig. 2. The dimensions were selected so that the antenna was amenable to theoretical analysis.¹³ Reflection coefficient and admittance measurements were made during re-entry utilizing a bidirectional coupler and a four-probe strip-line unit. The S-band antenna performed diagnostic measurements over the entire data period, whereas the Langmuir probes were retracted at 200,000 ft because of aerodynamic heating. Peak electron density and profile were inferred by comparing the admittance measurements with theoretical calculations. These data are not presented here, but are available elsewhere.¹⁴

Injection Experiment Results and Discussion

1. Electrostatic Probe Measurement

a. Effects of injection on probe data

This section presents a glimpse of the effects of injection on the electrostatic probe data. Details of the electrostatic probes, the data obtained, and the method of data reduction are not given here, but can be obtained elsewhere.^{4,12}

Figure 3 shows a plot of ion current as a function of time and altitude for a single fixed-bias probe. The buildup in plasma density with decreasing altitude along with the reduction associated with each injection pulse is apparent on this figure.

The effects of injection as a function of distance into the flowfield are illustrated by plotting ion density level of each fixed-bias probe as a function of its radial location. Such a plot showing levels with no injection, water injection, and electrophilic injection is shown in Fig. 4.[†]

Such electrostatic probe data are under analysis to evaluate the relative effectiveness of water and Freon E-3, and to determine the effective distribution of injectants in the flowfield.

[†] Freon E-3 fixed bias data do not show complete effects on Freon E-3 alleviation. These analyses are incomplete as yet, but are discussed in more detail.¹²

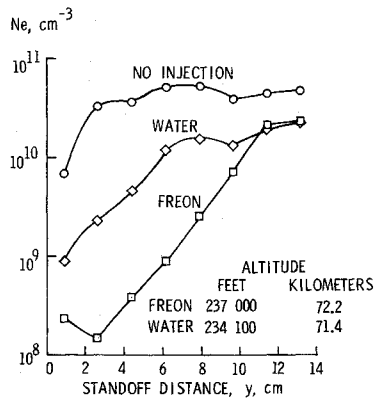


Fig. 4 Effects of injection on electrostatic probe ion density data (high mass-flow-rate injection cycle 3).

b. Penetration of injectants

As discussed in the previous section, electrostatic probe profile data provide a measurement of penetration depth of injected fluids. To obtain this depth, one merely compares the probe profile during injection to the corresponding profile with no injection to determine the depth at which plasma density reduction fades. A comparison of penetration depths so obtained using fixed-bias electrostatic data is shown in Fig. 5. Shown in this figure for comparison are calculated penetration depths and penetration requirements to quench below given N_e (electron density) levels.¹² Fixed-bias probe data appear to be insensitive to penetration depth for the first two cycles, and the probes are retracted after five cycles. Data from the remaining three cycles show reasonable agreement with calculated penetration levels based on the wind-tunnel correlation.⁹ The exception is for low water flow rates which are, in general, higher than predictions.

2. Signal Strength Measurements

a. Attenuation and recovery

Occurrence of attenuation and blackout for the various frequencies of the ground track stations are given in Table 1. The onset of VHF attenuation was somewhat obscured by material injection which had commenced prior to VHF blackout. The altitude of emergence of blackout varied between 89,000 ft and 67,000 ft, depending on signal frequency and receiving stations

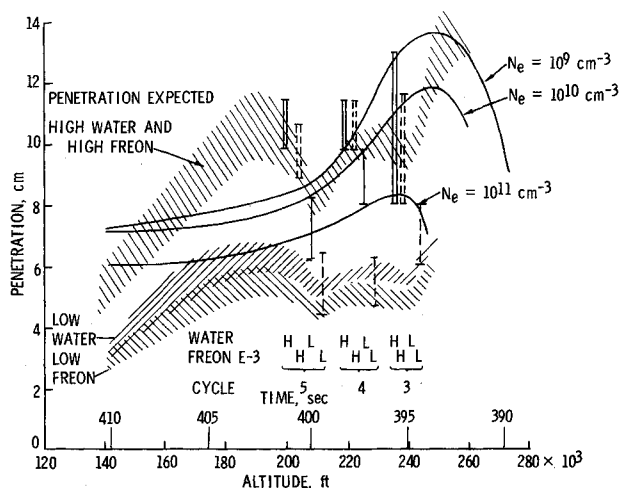


Fig. 5 Comparison of penetration measured by electrostatic probes with calculated penetration. (Probe-measured penetrations are shown as vertical bars, with key to injection pulses directly below.)

Table 1 Blackout times and altitudes

| Station | Signal frequency, MHz | Altitude at beginning of attenuation ft | Altitude at beginning of attenuation km | Altitude at signal blackout ft | Altitude at signal blackout km | Altitude at emergence from blackout ft | Altitude at emergence from blackout km |
|---------------------|-----------------------|---|---|--------------------------------|--------------------------------|--|--|
| Bermuda | 230.4 | 269,875 | 82.258 | 248,865 | 75.854 | 84,883 | 25.872 |
| | 259.7 | 272,079 | 82.930 | 246,081 | 75.005 | 79,502 | 24.232 |
| | 3348 | 227,613 | 69.376 | 218,547* | 66.613 | 66,624* | 24.478 |
| | 5800 | 201,073 | 61.287 | 190,688 | 58.122 | 73,515 | 22.407 |
| | 9210 | 182,265 | 55.554 | 143,050 | 43.602 | 68,305 | 20.819 |
| Aria Aircraft | 230.4 | 268,514 | 81.843 | 249,577 | 76.071 | 75,921* | 23.141 |
| | 259.7 | 270,912 | 82.574 | 247,506 | 75.440 | 67,252* | 20.498 |
| USNS range receiver | 230.4 | 271,170 | 82.653 | 249,124 | 75.933 | 88,495 | 26.973 |
| | 259.7* | 271,170 | 82.653 | 249,124* | 75.933 | Never recovered | |
| USS vanguard | 230.4 | 278,489 | 84.883 | 248,671* | 75.795 | 88,952 | 27.113 |
| | 259.7 | 279,136 | 85.081 | 248,671* | 75.795 | 78,312 | 23.869 |
| | 5800 | from signal strength | | 247,052 | 75.301 | 244,138* | 74.413 |
| | 5800 | from tracking signals | | 247,052 | 75.301 | 234,097 | 71.353 |
| | | | | | | 167,437 | 51.035 |

* Accuracy in question due to either 1) slow response, 2) signal recovery at onset of attenuation, or 3) tracking accuracy.

and was probably a function of tracking accuracy, signal margin, and aspect angle. Onset of blackout at VHF preceded that at S-band by 30,000 ft, C-band by 60,000 ft, and X-band by 105,000 ft. The advantage of using a high-frequency carrier signal is again demonstrated by the X-band system, which was blacked out for 75,000 ft, compared to approximately 170,000 ft for the VHF system.

Signal strength measurements and other data are shown for several frequencies received at Bermuda in Fig. 6. Directly below the electrostatic probe trace (discussed earlier) is a typical signal strength record at 259.7 MHz, the primary RF system for the injection experiment. The wave-form of the injection programmer is also shown to give the approximate times of injection. Attenuation begins at approximately the beginning of injection and blackout occurs at about the end of cycle 2, as previously noted. Signal recovery is seen throughout the entire injection period, indicating water and Freon E-3 both function well in reducing radio blackout. However, during the last two injection cycles, first the low and the high recovery levels decrease. These decreases correspond to altitudes where injectant penetration is expected to decrease.

S-band signal strength is modulated by roll rate of the spacecraft, since the antenna has about a 30° beam width. Recovery of transmitted signals from blackout require the injection pulses to occur when the S-band antenna is pointed at the receiving antenna and so not every injection pulse produces recovery. However, the corresponding plot of reflected signal (Fig. 6)

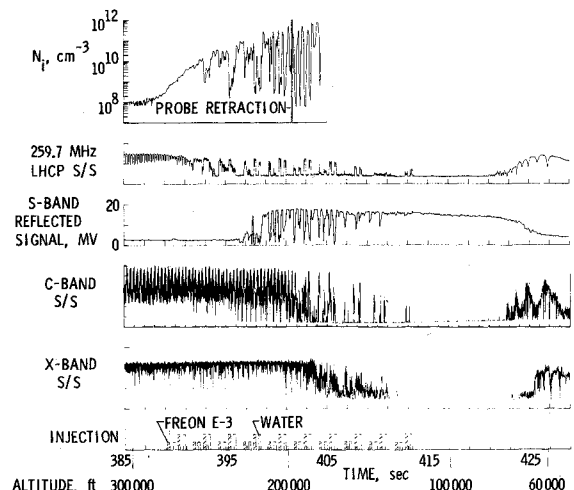


Fig. 6 RAM C-III signal strength (S/S) and other data.

Table 2 Attenuation and reflection for the RAM C-III

| Frequency, MHz | Critical, N_e , $1/\text{cm}^3$ |
|----------------|-----------------------------------|
| 259.7 | 8.4×10^8 |
| 3348 | 1.4×10^{11} |
| 5800 | 4.2×10^{11} |
| 9210 | 1.05×10^{12} |

indicates S-band signal is being relieved almost every time injection occurs.

C-band signal attenuation (Fig. 6, trace 4) onset occurred at about 201,000 ft and blackout occurred at 190,700 ft. Signal recovery is seen from cycle 6 to the end of injection, and recovery diminishes during the last three cycles. These results show that fluid was dispersed around the spacecraft to at least the C-band antenna location, about 30° off the injection axis.

X-band signal strength during the re-entry attenuation period is shown in the fifth trace of Fig. 6. Partial attenuation of the signal occurs from 182,000 ft altitude to signal blackout at 143,000 ft. This partial attenuation is probably due to the presence of sodium and potassium impurities in the ablation products of the flowfield. Signal recovery during the blackout period due to fluid injection is apparent for injection cycles 7–10.

An interesting check for consistency of the RAM C-III data may be obtained using the data of Fig. 6. The onset of attenuation and reflection at a given frequency occurs approximately at the onset of critical density which has been computed in Table 2 using the formula $N_e = (1.24 \times 10^{-8})f^2$.

The densities agree well with the probe measured values at the beginning of attenuation for each frequency. Inferred S-band electron density,¹⁴ not shown here, also compares well with these measurements. Further, injection produces consistent effects on all systems. Hence, there is a one-to-one correspondence between densities inferred by the probes and the response of the VHF, S-band, C-band, and X-band systems.

b. Comparison of RAM C-III signal recovery with RAM C-I recovery

As reported, signal recovery on the RAM C-I flight was below design estimates.² In order to evaluate progress in our understanding of injection techniques, a comparison between the effects of water injection on RAM C-I and RAM C-III is made in Fig. 7. (This comparison is allowable since the spacecraft configuration and entry trajectory were practically identical.) Shown in this figure are paired plots of 259.7 MHz signal for both flights being attenuated and finally blacked out, with attenuation onset on RAM C-III occurring about 7000 ft later than on RAM C-I. Vertical lines indicate signal recovery for RAM C-I, while RAM C-III data are indicated by lines paired between actual measurements of signal recovery. On some pulses, a narrow spike of signal recovery to a much greater level was observed, and these levels are indicated separately from regular signal recovery. The spiking phenomenon was observed in both flights, and appears

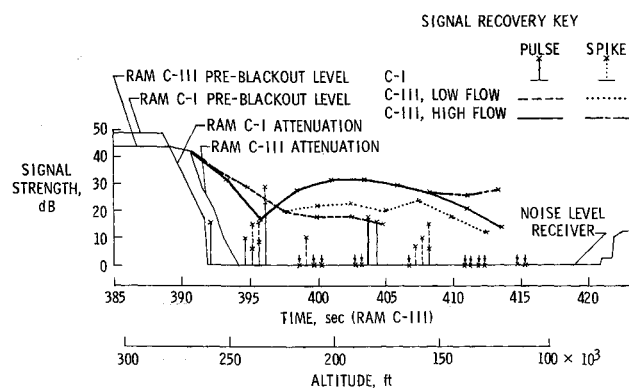


Fig. 7 Comparison of blackout alleviation due to water injection on the RAM C-I and RAM C-III flights at 259.7 MHz.

to be a transient effect when some injectant parameter is momentarily optimized.^{2,12}

Except for one point at about 235,000 ft, signal recovery for RAM C-III is 10–30 db greater in strength than RAM C-I. The RAM C-III water recovery was especially superior for the high flow rate; but even the low flow rate, which was expected to penetrate insufficiently, produced consistently higher signal strength of from 5 to 15 db. Another significant difference is that nearly all the RAM C-III pulses produced observable recoveries, but many RAM C-I pulses produced no noticeable effect. Hence, recovery produced by water injection during RAM C-III was significantly improved over the previous experiment. This improvement is underscored with the fact that RAM C-I flow rates were about three times higher than RAM C-III levels. The signal recovery data and the inferred penetration measurements previously shown indicate that injection system design using the method of RAM C-III⁹ is a significant improvement over previous methods.

c. Comparison of relative alleviation due to water and Freon E-3 injection during the RAM C-III flight

A primary objective of the RAM C-III injection experiment was the comparison of the relative blackout alleviation produced by water and Freon E-3 injection. Figure 8 shows a plot of the relative signal recovery due to injection, observed on 259.7 MHz (the prime injection experiment antenna), received at Bermuda. These data were from the diversity combiner, and were used because they seem to minimize the effects of receiver antenna polarization. The figure has the same general format as the previous one; the preattenuation level is shown, followed by onset of attenuation, and finally blackout to the receiver noise level.

Signal recovery due to injection of water and Freon E-3 are indicated by pairings between actual signal recovery levels. Recovery levels due to spiking are indicated separately. The recovery due to water was discussed in the previous section, and as indicated there, was significantly greater than corresponding results during RAM C-I. It is noted, however, from Fig. 8, that alleviation due to Freon E-3 injection for both high and low flow levels is greater than water up to the end of cycle 5. Recovery levels for water and Freon E-3 appear to be about equal for subsequent injectant cycles. Hence, the apparent superiority of Freon E-3 over water in radio blackout alleviation has been demonstrated for 259.7 MHz down to altitudes of about 200,000 ft. Analysis of S-band, C-band, and X-band recovery^{15,16} show that this superiority also exists at other frequencies and at other antenna locations. However, data at these higher frequencies indicate that Freon E-3 alleviation is superior throughout the injection period. The actual mechanism responsible for this superiority is under investigation by NASA.¹⁷

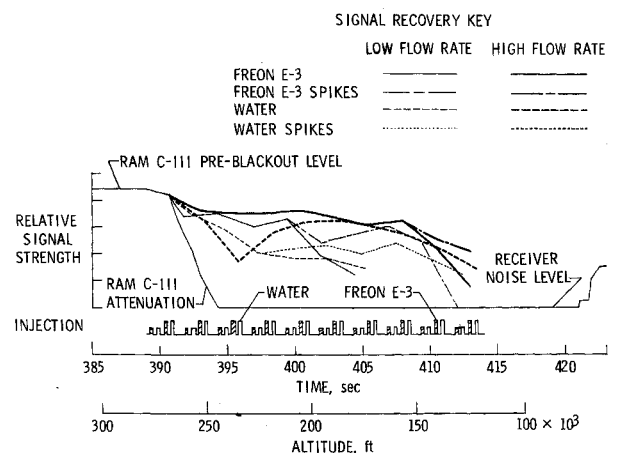


Fig. 8 Comparison of alleviation due to Freon E-3 with water during the RAM C-III injection experiment.

Conclusions

Based on the data from the RAM C-III flight and that presented herein, the following conclusions can be made. 1) Penetration predicted by wind-tunnel scale-model tests and correlations are in general agreement with probe measured effective penetration. 2) Electron densities measured with the S-band antenna and the electrostatic probe compare favorably with densities inferred from observed signal attenuation onset. 3) Water injection caused considerably greater signal recovery on 259.7 MHz during RAM C-III than on RAM C-I, using less than one-third the mass flow rates. 4) Freon E-3 alleviation on 259.7 MHz is superior to water at altitudes above 200,000 ft, and approximately equal at lower altitudes for conditions of RAM C-III. Alleviation at other frequencies indicated Freon E-3 was superior throughout the injection period.

References

- ¹ Schroeder, L. C., *RAM Flight Test Results and Conclusions*, NASA SP-52, 1964.
- ² Akey, N. D. and Cross, A. E., "Radio Blackout Alleviation and Plasma Diagnostic Results From a 25,000 Foot-Per-Second Blunt-Body Reentry," TN D-5615, 1970, NASA.
- ³ Grantham, W. L., "Flight Results of a 25,000 Foot-Per-Second Reentry Experiment Using Microwave Reflectometers to Measure Plasma Electron Density and Standoff Distance," TN D-6062, 1970, NASA.
- ⁴ Kang, S.-W., Jones, W. L., Jr., and Dunn, M. G., "Theoretical and Measured Electron Density Distributions for the RAM Vehicle at High Altitudes," *AIAA Journal*, Vol. 11, No. 2, Feb. 1973, pp. 141-149.
- ⁵ Kurzius, S. C. and Ellison, R., "Effect of Water Droplets on Reentry Plasma Sheaths," CR-66149, 1965, NASA.
- ⁶ Kurzius, S. C., Raab, F. H., and Revolenski, R. L., "Ionization Suppression in High Temperature, Low Pressure Plasma by Electrophilic Vapors and Sprays," CR-1701, 1970, NASA.
- ⁷ Cuddihy, W. F., Beckwith, I. E., and Schroeder, L. C., "Flight Test and Analysis of a Method for Reducing Radio Attenuation During Hypersonic Flight," TM X-1331, 1967, NASA.
- ⁸ Schroeder, L. C. and Russo, F. P., "Flight Investigation and Analysis of Alleviation of Communications Blackout by Water Injection During Gemini 3 Reentry," TM X-1521, 1968, NASA.
- ⁹ Weaver, W. L., "Multiple-Orifice Liquid Injection Into Hypersonic Air Streams and Application to RAM C-III Flight," TM X-2486, 1972, NASA.
- ¹⁰ Crowe, R. W. and Kilpatrick, W. D., "A Fundamental Study of Electrophilic Gases and Plasma Quenching," CR-66206, 1968, NASA.
- ¹¹ Jones, W. L., Jr. and Cross, A. E., "Electrostatic-Probe Measurements of Plasma Parameters for Two Reentry Flight Experiments at 25,000 Feet Per Second," TN D-6617, 1972, NASA.
- ¹² Schroeder, L. C., Jones, W. L., Jr., Swift, C. T., and Cross, A. E., "Radio Blackout Alleviation by Fluid Injection and Plasma Measurements During the RAM C-III Reentry at 25,000 Ft/Sec," TM X-2563, 1972, NASA.
- ¹³ Bailey, M. C. and Swift, C. T., "Input Admittance of a Circular Waveguide Aperture Covered by a Dielectric Slab," *IEEE Transactions on Antennas and Propagation*, Vol. AP-16, July 1968, pp. 386-391.
- ¹⁴ Schroeder, L. C., Swift, C. T., Akey, N. D., and Beck, F. B., "Material Injection Alleviation and Plasma Diagnostic Measurements During the RAM C-III Flight," AIAA Paper 72-690, Boston, Mass., 1972.
- ¹⁵ Britt, C. L., Ruedger, W. H., Wisler, M. M., and Sheppard, E. L., "Evaluation of RAM C-III X-Band and S-Band Signal Strength Data," CR-112039, 1972, NASA.
- ¹⁶ Maestre, N. E., "Radio Attenuation Measurements, Series C, Flight III," CR-112013, 1972, NASA.
- ¹⁷ Pergament, H. S., Mikatarian, R. R., and Kurzius, S. C., "Prediction of Electron Concentration Reductions in Reentry Flow Fields Due to Electrophilic Liquid and Water Injection," AIAA Paper 72-670, Boston, Mass., 1972.